Dimensional dependence of phase transitions in explosive percolation

Woosik Choi, Huiseung Chae, Soon-Hyung Yook, and Yup Kim*
Department of Physics and Research Institute for Basic Sciences, Kyung Hee University, Seoul 130-701, Korea
(Received 25 April 2014; published 20 August 2014)

To understand the dependence of phase-transition natures in explosive percolations on space dimensions, the number $n_{\rm cut}$ of cutting bonds (sites) and the fractal dimension $d_{\rm CSC}$ of the critical spanning cluster (CSC) for the six different models introduced in Phys. Rev. E **86**, 051126 (2012) are studied on two- and three-dimensional lattices. It is found that $n_{\rm cut}(L \to \infty) = 1$ for the intrabond-enhanced models and the site models on the two-dimensional square lattice with lattice size L. In contrast, $n_{\rm cut}$ for the intrabond-suppressed models scales as $n_{\rm cut} \simeq L^{d_{\rm cut}}$ with $d_{\rm cut} = 1$. $d_{\rm CSC} = 2.00(1)$ is obtained for the intrabond-enhanced models and the site models, while $d_{\rm CSC} = 1.96(1)(< 2)$ is obtained for the intrabond-suppressed models in two dimensions (2D). These results strongly support that the intrabond-enhanced models and the site models undergo the discontinuous transition in 2D, while the intrabond-suppressed models do the continuous transition in 2D. On the three-dimensional cubic lattice, we find that $d_{\rm cut} > 0$ and $d_{\rm CSC} = 2.8(1)(< 3)$ for all six models, which indicates that the models undergo the continuous transition. Based on the finite-size scaling analyses of mean cluster size and order parameter, all six models in 3D show nearly the same critical phenomena within numerical errors.

DOI: 10.1103/PhysRevE.90.022123 PACS number(s): 05.70.Fh, 64.60.ah

I. INTRODUCTION

Since Achlioptas, D'Souza, and Spencer [1] suggested an explosive percolation model, there have been intensive studies on explosive percolations. The Achlioptas model [1] was originally argued to show the discontinuous phase transition by suppressing the growth of large clusters [1–3]. The explosive percolation models triggered intensive studies to understand transition natures [2–17]. However, subsequent studies have proved that the transition for the explosive percolations is continuous on the complete graph and the Bethe lattice [4–8]. Therefore, the phase transition for the explosive percolations is physically established to be continuous in the mean-field level or in higher dimensions.

In contrast, the transition nature for the explosive percolations in lower dimensions is still not fully understood. Especially, in two dimensions (2D), there still has been controversy between the continuous transition [7,9] and the discontinuous transition [3,10–17]. The controversy should come from ambiguity in the details of explosive percolation models on lattices. In this context, we have established a complete set of explosive percolation models on lattices to find out whether the transition nature depends on the details of a given model [16]. By studying the cluster-size distribution, the second largest cluster, and the finite-size scaling (FSS) analyses, it has been found that the intrabond-enhanced models and the site models in 2D show the discontinuous transition, whereas the intrabond-suppressed models in 2D show the continuous transition [16]. Furthermore, there have been few studies in moderate dimensions like three or four. To understand transition natures completely including the upper critical dimension d_c [4], one should study the dimensional dependence of transition natures.

Recently, an interesting relevant research result has been reported [17]. In Ref. [17], by controlling the growth of the spanning cluster by cutting (or red) bonds, the percolation transition can be made to be discontinuous. Here, a cutting bond means the bond which would disconnect the spanning cluster if it is removed. Therefore, it is an important study to investigate whether the specific explosive percolation models inherently avoid cutting bonds or not. If a model avoids cutting bonds naturally, the model should show the discontinuous transition. Otherwise, the model undergoes the continuous transition. The physical mechanism to form cutting bonds should depend on the connectivity of the base structure or on the dimension of the base lattice. Thus it is also very interesting to study the dependence of the number of cutting bonds on the dimension in a percolation model.

For this purpose, we investigate structural properties of critical spanning clusters of the explosive percolation models [16] on two-dimensional square and three-dimensional cubic lattices. Especially, the dependence of the number $n_{\rm cut}$ of cutting bonds on lattice size L is measured. The fractal dimensions $d_{\rm CSC}$ of critical spanning clusters are also measured. From these measurements, we first confirm transition natures of the models in 2D shown by different methods [16]. It is found that $n_{\rm cut}$ decreases as L increases and $d_{\rm CSC} = 2$ in the intrabond-enhanced models and the site models on the square lattice. These results strongly support the discontinuous transition. In the intrabond-suppressed models which show the continuous transition in 2D, the connectedness length exponent ν is numerically shown to satisfy the relation $\nu = 1/d_{\rm cut}$ [18–20]. From measured $d_{\rm CSC}$, the scaling relation $\beta/\nu = d - d_{\rm CSC}$ [21] is also numerically confirmed, where β is the critical exponent of the order parameter. In contrast, we find that $n_{\rm cut}$ increases as L increases in all six models on the cubic lattice. Furthermore, $d_{\rm CSC}$ of all the models in 3D satisfies the relation $\beta/\nu = d - d_{\rm CSC}$. Thus all the models show the continuous transition in 3D regardless of the details of the models. The critical phenomena of the models in 3D are also analyzed by using FSS ansatz for the average size $S(p,L)$ of finite clusters and the order parameter $P_\infty(p,L)$. From the analyses, it is numerically shown that the critical phenomena of all the models in 3D are nearly the same.

*ykim@khu.ac.kr

II. MODELS

The explosive percolation models in cubic lattices considered in this paper have already been defined in Ref. [16]. For clarity purposes let's explain them briefly here. There are two fundamental percolation models on lattices [21], the site percolation and the bond percolation. Initially, all the sites (or bonds) of a lattice are unoccupied. The percolation transition is considered by occupying sites (or bonds) using the following process.

In a unit growth process of the explosive site percolations, two vacant sites A and B are randomly selected. Let $\{s_{A_i}\}$ ($\{s_{B_j}\}$) be the sizes of n_A (n_B) clusters which would be connected by occupying the site A (B). In the d-dimensional cubic lattice n_A (n_B) is at most $2 \times d$. In the site model with a product rule (SP model), the site A is occupied if $1 \times \prod_{i=1}^{n_A} s_{A_i} < 1 \times \prod_{i=1}^{n_B} s_{B_i}$. Otherwise, the site B is occupied. Similarly, in the site model with a sum rule (SS model), the site A is occupied if $(1 + \sum_{i=1}^{n_A} s_{A_i}) < (1 + \sum_{j=1}^{n_B} s_{B_j})$.

Four explosive bond percolation models also have been considered in Ref. [16]. First two unoccupied bonds a and b are randomly selected. If the bond a is an interbond which connects two clusters of sizes s_{a1} and s_{a2}, then the product ξ_a and the sum σ_a are clearly defined as $\xi_a \equiv s_{a1} \times s_{a2}$ and $\sigma_a \equiv s_{a1} + s_{a2}$, respectively. If the bond is an intrabond, it internally connects two sites in the same cluster and there may exist some ambiguities to define the product and the sum. Thus ξ_a can be defined in two different ways. One is $\xi_a \equiv s_{a1} \times 1$ (bond product type 1 model: BP1 model). The other is $\xi_a \equiv s_{a1} \times s_{a1}$ (bond product type 2 model: BP2 model). The product ξ_b for bond b is defined in the same way. The sum σ_a is defined similar to $\sigma_a \equiv s_{a1} + 0$ (bond sum type 1 model: BS1 model) or $\sigma_a \equiv s_{a1} + s_{a1}$ (bond sum type 2 model: BS2 model). Then, occupy the bond a if $\xi_a < \xi_b$ ($\sigma_a < \sigma_b$). Otherwise, occupy the bond b. The physical meanings of these models are that the type 1 (BP1 and BS1) models are intrabond-enhanced models and type 2 (BP2 and BS2) models are intrabond-suppressed models.

III. STRUCTURAL PROPERTIES OF SPANNING CLUSTER IN 2D

As the cluster grows, there should occur a spanning cluster which connects the top and the bottom of the lattice (see Fig. 1). The spanning cluster which occurs at the smallest (critical) fraction p_c of occupied bonds (sites) is the critical spanning cluster (CSC). In low-dimensional lattices, the fraction of sites in CSC of the infinite-sized lattice can be regarded as the order parameter P_∞ of the percolation transition [21].

To understand transition natures of the explosive percolation models, we first investigate physical properties of the cutting bond (site) of CSC for each model. The cutting bond (site) would disconnect CSC if it is removed (see Fig. 1). In ordinary (random) percolation which shows the continuous phase transition the number of cutting bonds (sites), $n_{\rm cut}$, scales as [18–21]

$$n_{\rm cut} \simeq L^{d_{\rm cut}}, \tag{1}$$

where $d_{\rm cut}$ is the fractal dimension of cutting bonds (sites). Furthermore, based on the node-link-blob picture of CSC, $d_{\rm cut}$ for ordinary percolation and Potts-correlated percolation is shown to exactly satisfy the relation [18–20]

$$d_{\rm cut} = 1/\nu \tag{2}$$

in any d, where ν is the connectedness length exponent [20]. Especially, on the two-dimensional square lattice, $d_{\rm cut} = 0.75$ as shown in Fig. 2(a) for ordinary percolations, which is one of the numerical evidences for the relation (2) [18]. In contrast, if the percolation transition is discontinuous, then it is expected that $n_{\rm cut}(L) \to$ finite const as $L \to \infty$.

The dependences of $n_{\rm cut}$ on L for the six models in 2D are shown in Figs. 2(b) and 2(c). All data in Fig. 2 is obtained from averaging over at least 10^3 realizations. As shown in Fig. 2(b), $n_{\rm cut}$ for the intrabond-enhanced (BP1 and BS1) models and the site (SP and SS) models monotonically decrease as L increases. If $n_{\rm cut}(L)$'s for these models are forced to fit the relation (1), one gets $d_{\rm cut} < 0$. This decreasing property of $n_{\rm cut}(L)$ means that $n_{\rm cut}(L \to \infty) = 1$. This result clearly supports the fact that two main relatively compact and large clusters merge to form CSC by occupying a bond (a site), which is a strong evidence for the discontinuous transition. This evidence is nearly identical to that for the discontinuous transition in Potts models with $q > 4$ in 2D, because $d_{\rm cut}$ of the models has been shown to go to zero [20]. This strong evidence also coincides with the result in Ref. [16] that both the intrabond-enhanced models and the site models in 2D show the discontinuous transition, which was based on the cluster-size distribution and the property of the second largest cluster.

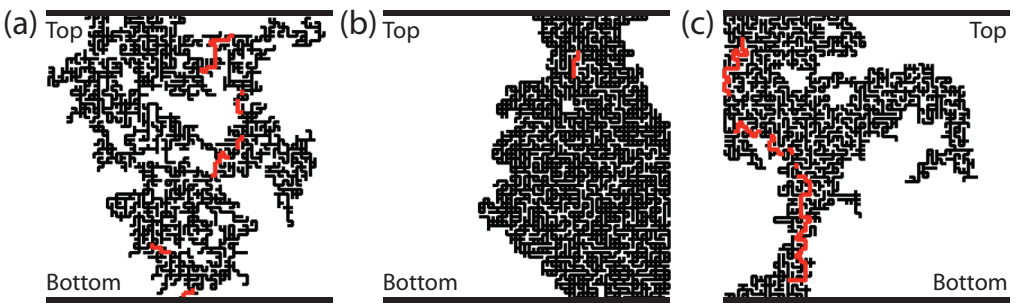

FIG. 1. (Color online) Critical spanning clusters (CSCs) on a two-dimensional square lattice with $L = 64$ (a) for ordinary percolations, (b) for the BP1 model, and (c) for the BP2 model. Black bonds are bonds in CSCs. Dark gray (red) bonds are cutting bonds. The distribution of cutting bonds in (a) and (c) spreads relatively widely in CSCs. But cutting bonds in (b) are extremely localized.

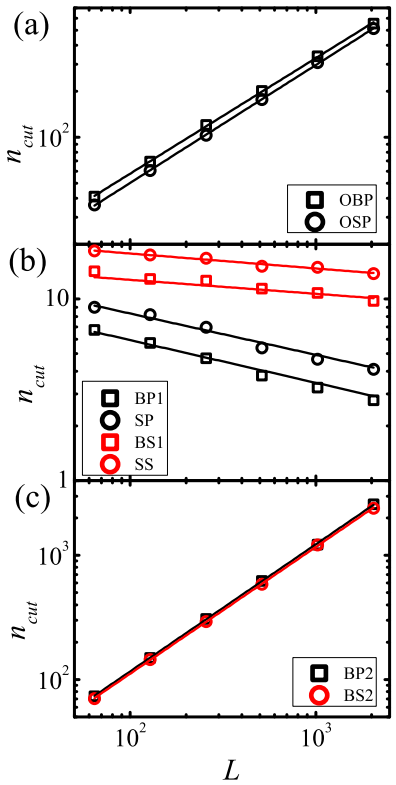

FIG. 2. (Color online) (a) Dependence of $n_{\rm cut}$ on the size L of the square lattice for ordinary bond percolation (OBP) and ordinary site percolation (OSP). By fitting to Eq. (1) $d_{\rm cut} = 0.75(1)$ is obtained for both the percolations. (b) The same plots for the BP1, BS1, SP, and SS models. Measured p_c are $p_c = 0.694(1)$ for the BP1 model, $p_c = 0.598(1)$ for the BS1 model, $p_c = 0.773(1)$ for the SP model, and $p_c = 0.692(1)$ for the SS model. (c) The same plots for the BP2 and BS2 models. Measured p_c are $p_c = 0.5266(1)$ for the BP2 model and $p_c = 0.5270(1)$ for the BS2 model. By fitting, $d_{\rm cut} = 1.00(1)$ is obtained for both the BP2 and BS2 models.

In contrast, $n_{\rm cut}$ of the intrabond-suppressed (BP2 and BS2) models satisfy the relation (1) with $d_{\rm cut} > 0$ very well as shown in Fig. 2(c). From the data in Fig. 2(c), $d_{\rm cut} = 1.00(1)$ is obtained for both the BP2 [14] and BS2 models. $\nu = 1.00(2)$ was obtained by FSS analyses of the order parameter, the susceptibility, and the cluster-size distribution for the BP2 and BS2 models [16]. Thus the relation (2) is also valid for the intrabond-suppressed models in 2D. The physical property of the cutting bond strongly supports that the intrabond-suppressed models show the continuous transition in 2D.

In Ref. [17], by avoiding or suppressing cutting bonds, the percolation transition can be made to be discontinuous. In the intrabond-enhanced models in 2D, the avoidance of cutting bonds occurs naturally and inherently and is the main physical mechanism for the discontinuous transition. In contrast, the avoidance is not so prominent in the intrabond-suppressed models.

To confirm transition natures in another way the fractal dimension, $d_{\rm CSC}$, of CSCs is also measured. In ordinary percolations, the number of sites in CSC, $n_{\rm CSC}$, scales as [21]

$$n_{\rm CSC} \simeq L^{d_{\rm CSC}}, \tag{3}$$

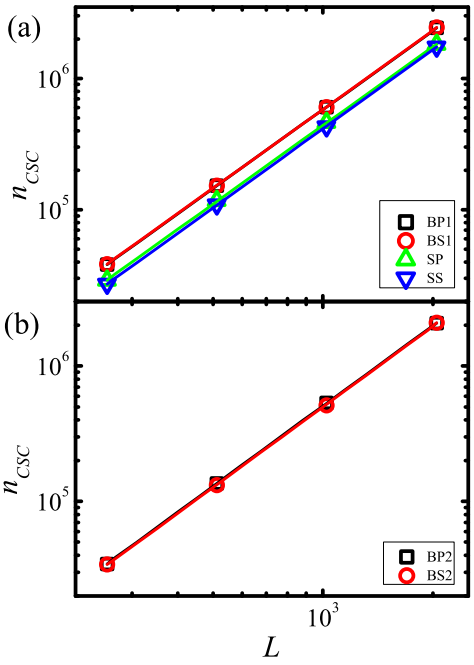

FIG. 3. (Color online) (a) Dependence of $n_{\rm CSC}$ on L in 2D for the intrabond-enhanced (BP1 and BS1) models and the site (SP and SS) models. By fitting to Eq. (3), $d_{\rm CSC} = 2.00(1)$ are obtained for the four models. (b) The same plots for the intrabond-suppressed (BP2 and BS2) models. $d_{\rm CSC} = 1.96(1)$ are obtained for the two models.

with $d_{\rm CSC} = 91/48$ in 2D [21]. Figure 3 shows that $n_{\rm CSC}$ satisfies Eq. (3) very well for all six models. For the intrabond-enhanced models and the site models, we find $d_{\rm CSC} = 2.00(1)$. This result $d = 2 = d_{\rm CSC}$ physically means that P_∞, defined as the fraction of sites in CSC, is a nonzero constant k at $p = p_c$ in the limit $L \to \infty$ as $P_\infty = n_{\rm CSC}/L^d = kL^2/L^2 = k$. Thus the order parameter P_∞ is sure to jump from zero to a nonzero value at $p = p_c$. In addition, it is well known that CSC has a compact structure when the transition is discontinuous near $p = p_c$ [17]. Therefore, the result $d = d_{\rm CSC}$ for the intrabond-enhanced models and the site models in 2D is also strong evidence for the discontinuous transition.

In contrast, for the intrabond-suppressed models, $d > d_{\rm CSC} = 1.96(1)$ is obtained from Fig. 3(b). Thus $P_\infty \simeq \lim_{L\to\infty} n_{\rm CSC}/L^d = 0$ at $p = p_c$, which implies the continuous transition. Furthermore, P_∞ is expected to scale at $p = p_c$ as

$$P_\infty \sim L^{-\beta/\nu} = L^{-(d-d_{\rm CSC})}, \tag{4}$$

when the transition is continuous [21]. From the results $d_{\rm CSC} = 1.96(1)$ and $\nu = 1/d_{\rm cut} = 1.00(2)$, $\beta = 0.04(1)$ is obtained for the BP2 and BS2 models, and this β value is identical to that obtained from FSS analysis of $P_\infty(p,L)$ [16].

IV. STRUCTURAL PROPERTIES OF SPANNING CLUSTER IN 3D

To understand the dependence of transition natures on the lattice dimension, the structural properties of CSCs for the six models on a three-dimensional simple cubic lattice are also studied.

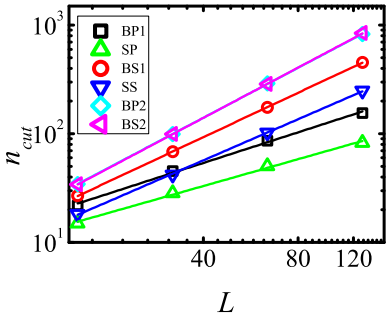

FIG. 4. (Color online) Dependence of $n_{\rm cut}$ on the size L for six models in 3D. Measured p_c's are $p_c = 0.3474(1)$ for the BP1 model, $p_c = 0.4405(1)$ for the SP model, $p_c = 0.3314(1)$ for the BS1 model, $p_c = 0.4280(1)$ for the SS model, $p_c = 0.3221(1)$ for the BP2 model, and $p_c = 0.3175(1)$ for the BS2 model. By fitting to Eq. (1), $d_{\rm cut} = 0.95(3)$ for the BP1 and SP models, $d_{\rm cut} = 1.35(3)$ for the BS1 and SS models, and $d_{\rm cut} = 1.53(1)$ for the BP2 and BS2 models are obtained, respectively.

In contrast to $n_{\rm cut}$'s in 2D, $n_{\rm cut}$'s of all six models in 3D satisfy Eq. (1) with $d_{\rm cut} > 0$. As shown in Fig. 4, $d_{\rm cut} = 0.95(3)$ for the BP1 and SP models and $d_{\rm cut} = 1.35(3)$ for the BS1 and SS models are obtained, respectively. The result $d_{\rm cut} > 0$ for the intrabond-enhanced models and the site models physically means that transition nature in these models is changed from the discontinuous transition to the continuous transition as d increases from $d = 2$ to $d = 3$. As d increases, the connectivity of underlying structures increases and the intrabond enhancement may not be relevant to make the inherent avoidance of cutting bonds (sites) in 3D. Thus this result also physically implies why the explosive percolation shows the continuous transition in the mean-field level and on the complete graph [4–8]. Another physical fact which can be seen from results for $d_{\rm cut}$ in 3D is the bond-site duality. As shown in Fig. 4, $d_{\rm cut}$ for the BP1 model is the same as that for the SP model. $d_{\rm cut}$ for the BS1 model is also the same as that for the SS model. Therefore, the bond-site duality which has been shown in 2D [16] still sustains in 3D.

In Fig. 5, we display the measured $n_{\rm CSC}$ in 3D. For all six models, $d > d_{\rm CSC} = 2.8(1)$ are obtained from the data in Fig. 5. Thus $P_\infty \simeq \lim_{L\to\infty} n_{\rm CSC}/L^d = 0$. This result provides another clear evidence that the intrabond-enhanced models and the site models undergo the continuous transition in 3D. Here, the bond-site duality in 3D [16] can also be verified.

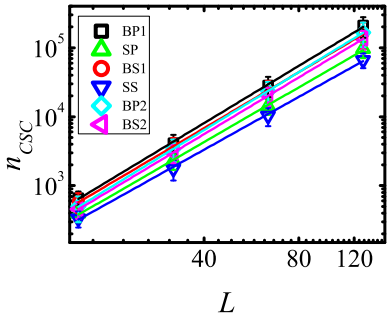

FIG. 5. (Color online) Dependence of $n_{\rm CSC}$ on L in 3D for six models. By fitting to Eq. (3), $d_{\rm CSC} = 2.8(1)$ for the six models.

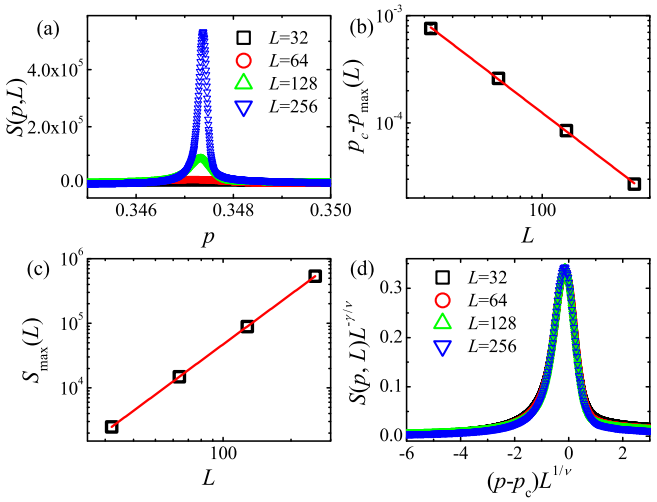

FIG. 6. (Color online) (a) Plot of $S(p,L)$ against L for the BP1 model in 3D. (b) Plot of $[p_c - p_{\rm max}(L)]$ against L. The solid line represents the relation $p_c - p_{\rm max}(L) \sim L^{-1/\nu}$ with $p_c = 0.3474(1)$ and $1/\nu = 1.6(1)$. (c) Plot of $S_{\rm max}(L)$ against L. The solid line denotes $S_{\rm max}(L) \sim L^{\gamma/\nu}$ with $\gamma/\nu = 2.57(3)$. (d) The scaling collapse of $S(p,L)$ with $p_c = 0.3474$, $\gamma/\nu = 2.57$, and $1/\nu = 1.6$.

Since the models show the continuous transition in 3D, the critical properties of the models are analyzed by FSS ansatz for the average size $S(p,L)$ of finite clusters and the order parameter $P_\infty(p,L)$. Until now, we have focused on the structural properties of CSC and thus simulations are carried out using the open boundary condition along the direction perpendicular to the top and bottom planes in the cubic lattice. However, $S(p,L)$ and $P_\infty(p,L)$ obtained from simulations with the open boundary condition do not satisfy FSS ansatz quite well. It is known that the inhomogeneity of the system increases when the open boundary condition is used in higher dimensions [22]. In this sense, $S(p,L)$ and $P_\infty(p,L)$ for FSS analyses are obtained from simulations using a periodic boundary condition to remove the inhomogeneity of a finite system and minimize systematic difference in accordance with the finite-size effect.

$S(p,L)$ for the BP1 model obtained from simulations is shown in Fig. 6(a). By fitting the relation $p_c - p_{\rm max}(L) \sim L^{-1/\nu}$ as Fig. 6(b), $1/\nu = 1.6(1)$ and $p_c = 0.3474(1)$ are obtained. Here, $p_{\rm max}(L)$ means the p at which $S(p,L)$ is maximal [21]. From the relation, $S_{\rm max} \sim L^{\gamma/\nu}$, of the maximal value of $S(p,L)$ [21], $\gamma/\nu = 2.57(3)$ is also obtained as shown in Fig. 6(c). $S(p,L)$ for the BP1 model satisfies FSS ansatz [21]

$$S(p,L) = L^{\gamma/\nu} f[(p - p_c)L^{1/\nu}], \tag{5}$$

very well with $\gamma/\nu = 2.57$, $1/\nu = 1.6$, and $p_c = 0.3474$ [see Fig. 6(d)].

$P_\infty(p,L)$ for the BP1 model obtained from simulations is shown in Fig. 7(a). From the relation $P_\infty(p_c,L) \sim L^{-\beta/\nu}$ [21] and $P_\infty(p_c,L)$ obtained from simulations, $\beta/\nu = 0.16(6)$ as the inset of Fig. 7(a). Figure 7(b) shows that $P_\infty(p,L)$ for the BP1 model also satisfies FSS ansatz [21]

$$P_\infty(p,L) = L^{-\beta/\nu} g[(p - p_c)L^{1/\nu}], \tag{6}$$

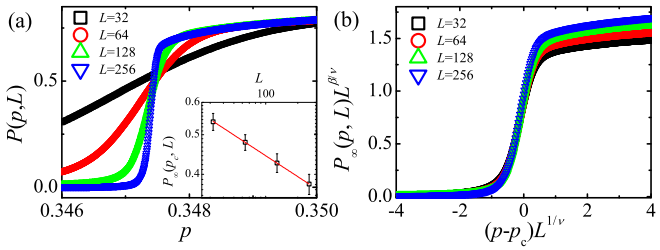

FIG. 7. (Color online) (a) Plot of $P_\infty(p,L)$ against L for the BP1 model in 3D. Inset: plot of $P_\infty(p_c,L)$ against L and the solid line represents the relation $P_\infty(p_c,L) \sim L^{-\beta/\nu}$ with $\beta/\nu = 0.16(6)$. (b) The scaling collapse of $P_\infty(p,L)$ with $p_c = 0.3474$, $\beta/\nu = 0.16$, and $1/\nu = 1.6$.

very well with $\beta/\nu = 0.16, 1/\nu = 1.6$, and $p_c = 0.3474$. Measured $\beta/\nu = 0.16(6)$ from the FSS ansatz is close to that obtained from the relation $\beta/\nu = d - d_{\rm CSC}$ [Eq. (4)] with $d_{\rm CSC} = 2.8(1)$ in Fig. 5. The critical probability $p_c = 0.3474(1)$ estimated from $S(p,L)$ and $P_\infty(p,L)$ for the BP1 model is nearly identical to that estimated from the analyses of CSC as shown in Fig. 5. The obtained exponents, $\beta/\nu = 0.16(6)$ and $\gamma/\nu = 2.57(3)$, satisfy the hyperscaling relation, $2\beta/\nu + \gamma/\nu = d$, quite well in 3D. We also obtain nearly the same exponents for the remaining five models as those for the BP1 model. p_c depends on the details of the models. The measured p_c's in 3D are $p_c = 0.4405(1)$ for the SP model, $p_c = 0.3314(1)$ for the BS1 model, $p_c = 0.4280(1)$ for the SS model, $p_c = 0.3221(1)$ for the BP2 model, and $p_c = 0.3175(1)$ for the BS2 model, respectively. These results imply that all six models in 3D show the continuous transition. Furthermore, their critical phenomena are nearly the same in 3D.

However, the relation $d_{\rm cut} = 1/\nu$ is not valid for the models in 3D. The bonds in the explosive percolation models are not random but correlated and the relation (2) does not necessarily hold in higher dimensions.

V. SUMMARY AND DISCUSSIONS

In summary, we investigate the structural properties of CSC for the six explosive percolation models in 2D and 3D. In the intrabond-enhanced (BP1, BS1) models and the site (SP, SS) models in 2D, it is found that $n_{\rm cut}(L \to \infty) = 1$. This behavior of $n_{\rm cut}$ strongly supports the discontinuous transition in the BP1, BS1, SP, and SS models. Moreover, for these models, $d_{\rm CSC} = d = 2$ is measured. The result $d_{\rm CSC} = d = 2$ also strongly supports the discontinuous transition, because $P_\infty \sim n_{\rm CSC}/L^d \sim$ const at $p = p_c$ in the limit $L \to \infty$. Therefore, the transition for the intrabond-enhanced models and the site models in 2D should be discontinuous. In contrast, $d_{\rm cut} > 0$ and $d_{\rm CSC} < d = 2$ are measured for the BP2 and BS2 models in 2D. The numerical result $d_{\rm cut} = 1$ for the BP2 and BS2 models also coincides with $1/\nu$ obtained by the previous FSS analyses of the order parameter, the susceptibility, and the cluster-size distribution [16]. Furthermore, it is also found that $\beta = 0.04(1)$ obtained from $d - d_{\rm CSC} = \beta/\nu$ is also nearly identical to that obtained from the previous analysis [16]. Thus the intrabond-suppressed (BP2 and BS2) models should undergo the continuous transition in 2D.

The structural properties of the six models in 3D are also studied. The results $d_{\rm cut} > 0$ and $d > d_{\rm CSC}$ are obtained for all six models. Thus transitions in the models should be continuous in 3D. This result means that only the intrabond-enhancement cannot make the inherent avoidance of cutting bonds in 3D. Furthermore, $S(p,L)$ and $P_\infty(p,L)$ are measured to understand the critical phenomena of the six models in 3D. From the FSS ansatz, $\beta/\nu = 0.16(6)$, $\gamma/\nu = 2.57(3)$, and $1/\nu = 1.6(1)$ are obtained for the six models. The obtained exponents also satisfy the hyperscaling relation, $2\beta/\nu + \gamma/\nu = d$, quite well in 3D. These results imply that the critical phenomena of the six models in 3D are nearly the same.

As explained before, the natural or inherent suppression of cutting bonds (sites) does not act physically to make the transition discontinuous in three and higher dimensions. Thus, even in the intrabond-enhanced models, the higher connectivity in $d \geqslant 3$ is the main mechanism for the continuous transition. From the connectivity point of view one can also understand why the explosive percolation shows the continuous transition on the complete graph or in the mean-field level.

There has been only one paper discussing d_c of the explosive percolation [4]. From a renormalization-group theory [4] d_c of a certain variant of the Achlioptas, D'Souza, and Spencer model [1] was argued to be smaller than 3. In the explosive percolation models considered in this paper, the hyperscaling relation $2\beta/\nu + \gamma/\nu = d = 3$ still holds within the measurement errors in 3D. If $d_c < 3$, the hyperscaling relation would be $2\beta/\nu + \gamma/\nu = d_c < 3$. However, since the order-parameter exponent β is known to be very small for the explosive percolation models in the mean-field level [3–5,7–10,16], it should be very hard to determine d_c using the numerical simulations.

Our final comment is on the maximal length scale $L_{\rm max}$ that is chosen for the calculation of $d_{\rm cut}$. $L_{\rm max} = 2048 (N_{\rm max} = L_{\rm max}^2 = 2^{22})$ in 2D and $L_{\rm max} = 128 (N_{\rm max} = L_{\rm max}^3 = 2^{21})$ in 3D are used. These $L_{\rm max}$'s for the calculation of $d_{\rm cut}$ are somewhat smaller than $L_{\rm max} = 8192$ in 2D used for a modern paper on a percolation model [7] and for our previous measurements of the cluster-size distribution, the order parameter, and the susceptibility of all six models [16]. In 3D, $L_{\rm max} = 256$ can be easily used for the measurement of the order parameter and the susceptibility of all six models (see Figs. 6 and 7). However, to calculate $n_{\rm cut}$ of a CSC in simulation, the cluster determining algorithm such as the burning algorithm and the Hoshen-Kopelman algorithm [21] should be repeated times comparable to the system size. Therefore, using larger system sizes for $d_{\rm cut}$ is practically or computationally intractable. However, even for measurements of $d_{\rm cut}$'s using $L_{\rm max} = 2048$ in 2D and $L_{\rm max} = 128$ in 3D, $d_{\rm cut}$ and $d_{\rm CSC}$ are obtained with enough accuracy, because $n_{\rm cut}$ and $n_{\rm CSC}$ satisfy the power laws (1) and (3) very accurately as in Figs. 2–5.

ACKNOWLEDGMENTS

This research was supported by Basic Science Research Program through the National Research Foundation of Korea (NRF) funded by the Ministry of Science, ICT & Future Planning (Grants No. NRF-2013R1A1A2057791 and No. NRF-2012R1A1A2007430).

[1] D. Achlioptas, R. M. D'Souza, and J. Spencer, Science **323**, 1453 (2009).
[2] Y. S. Cho, J. S. Kim, J. Park, B. Kahng, and D. Kim, Phys. Rev. Lett. **103**, 135702 (2009).
[3] F. Radicchi and S. Fortunato, Phys. Rev. E **81**, 036110 (2010).
[4] R. A. da Costa, S. N. Dorogovtsev, A. V. Goltsev, and J. F. F. Mendes, Phys. Rev. Lett. **105**, 255701 (2010).
[5] H. K. Lee, B. J. Kim, and H. Park, Phys. Rev. E **84**, 020101(R) (2011).
[6] O. Riordan and L. Warnke, Science **333**, 322 (2011).
[7] P. Grassberger, C. Christensen, G. Bizhani, S.-W. Son, and M. Paczuski, Phys. Rev. Lett. **106**, 225701 (2011).
[8] H. Chae, S.-H. Yook, and Y. Kim, Phys. Rev. E **85**, 051118 (2012).
[9] N. Bastas, K. Kosmidis, and P. Argyrakis, Phys. Rev. E **84**, 066112 (2011).
[10] R. M. Ziff, Phys. Rev. E **82**, 051105 (2010).
[11] Y. Kim, Y. K. Yun, and S.-H. Yook, Phys. Rev. E **82**, 061105 (2010).
[12] S. S. Manna and A. Chatterjee, Physica A **390**, 177 (2011).
[13] N. A. M. Araújo, J. S. Andrade, Jr., R. M. Ziff, and H. J. Herrmann, Phys. Rev. Lett. **106**, 095703 (2011).
[14] J. S. Andrade, Jr., H. J. Herrmann, A. A. Moreira, and C. L. N. Oliveira, Phys. Rev. E **83**, 031133 (2011).
[15] W. Choi, S.-H. Yook, and Y. Kim, Phys. Rev. E **84**, 020102(R) (2011).
[16] W. Choi, S.-H. Yook, and Y. Kim, Phys. Rev. E **86**, 051126 (2012).
[17] Y. S. Cho, S. Hwang, H. J. Herrmann, and B. Kahng, Science **339**, 1185 (2013).
[18] A. Coniglio, Phys. Rev. Lett. **46**, 250 (1981).
[19] A. Coniglio, J. Phys. A: Math. Gen. **15**, 3829 (1982).
[20] A. Coniglio, Phys. Rev. Lett. **62**, 3054 (1989).
[21] D. Stauffer and A. Aharony, *Introduction to Percolation Theory*, 2nd ed. (Taylor & Francis, London and New York, 1994).
[22] D. P. Landau and Kurt Binder, *A Guide to Monte Carlo Simulations in Statistical Physics* (Cambridge University Press, Cambridge, England, 2000).